



SEISMIC PERFORMANCE OF FLEXURAL CONTROLLED SRC COMPOSITE COLUMNS IN EXISTING BUILDINGS

M. Farag⁽¹⁾, W. Hassan⁽²⁾

⁽¹⁾ Research Assistant, American University in Cairo, Egypt, mayer@aucegypt.edu

⁽²⁾ Visiting Assistant Professor, American University in Cairo, Egypt
Adjunct Assistant Professor, Housing & Building National Research Center, Cairo, Egypt, whassan@berkeley.edu

Abstract

This paper addresses experimentally the cyclic performance of older-type steel reinforced concrete (SRC) columns that resemble existing buildings and bridges of pre 1980s construction; prior to enforcing seismic details. Two flexural controlled test specimens representing exterior columns modeled based on a typical seismic design of a 20-story prototype gravity-designed existing building are constructed and tested under quasi-static cyclic loading with different axial compression load levels. The tested columns include non-seismic widely spaced hoops with 90 degree hooks; thus the columns are considered flexure and confinement deficient. Test parameters include target failure mode and axial load ratio. The tests aim to quantify existing SRC columns seismic strength and deformability along with a preliminary attempt to establish backbone curve recommendations. From performance-based engineering demand viewpoint, the results show very satisfactory drift capacity associated with low axial load ratio indicating no need for retrofit and limited drift capacity and early strength loss and stiffness degradation under high axial load ratio suggesting the need for retrofitting existing SRC flexural columns with high axial loads.

Keywords: SRC columns; composite; seismic assessment; existing buildings; non-ductile concrete.



1. Introduction

The existing building stock in many active seismic regions includes many seismically deficient buildings that were constructed prior to enforcing seismic details in the 1980s. Many existing buildings and bridges utilize SRC columns, with structural steel sections embedded in concrete, that are not seismically designed/detailed. Literature reveals a serious lack of knowledge on the behavior of SRC composite columns subjected to simulated seismic loading conditions. There are a small number of tests available to justify deriving definitive conclusions regarding the strength, deformability and seismic backbone curves for macro-modeling or retrofitting purposes. Numerical criteria to distinguish the seismic modes of failure of such columns are also absent. In addition, no information on the residual axial capacity of SRC composite columns following shear or flexural failure can be drawn from the few tests available in the literature due to premature test termination.

Ricles and Paboojian (1992) at University of California San Diego tested six SRC column specimens to quantify lateral stiffness, transverse shear resistance, level of concrete confinement, and the effectiveness of shear studs in resisting lateral loading. Chen et al. (2007) conducted an experimental study on twenty six specimens to study the seismic behavior of SRC composite members and their influence parameters. They used three steel section shapes and changed the parameters of axial load ratio, longitudinal steel ratio, steel section ratio, embedded steel section length, and transverse steel ratio. It is noteworthy that most of the tested specimens in these two studies resembled modern construction practices not the older ones. According to the results of these two studies, longitudinal bar buckling must be prevented to preserve the integrity of the member under cyclic action, the axial compression ratio is an important factor that affects the seismic behavior of steel concrete columns, hoop ratio is very significant in the seismic behavior of SRC columns, and the minimum value of the embedded depth of steel concrete composite column can be 2.5 times the section depth. No recommendations for the backbone curves or performance acceptance criteria were made in these studies. In the current paper, an experimental program consisting of two large-scale test specimens is conducted to address the seismic strength and deformation capacities along with residual axial capacity of flexural controlled SRC columns lacking seismic details.

2. Test Matrix and Material Properties

A 20 story prototype building mimicking gravity designed older construction was used to obtain the seismic demands on an existing flexural controlled exterior column. According to ACI 318-63, the composite column design equation does not differ from the current ACI 318-14 equation. However, the main difference is the steel section ratio, which is 5%-9% A_c (where A_c is gross concrete area) in older code versus 1%-3% A_c in ACI 318-14 code, and the longitudinal steel ratio, which is 2%-3% A_c in the older code instead of 1%-2% A_c in the modern one. Locally produced ready mixed concrete of 27 MPa cylinder characteristic strength was used to construct the test specimens. Actual yield strength of longitudinal steel bars and transverse hoops were 428 MPa and 516 MPa, respectively, while that of the steel section was 435 MPa.

The current tests aimed to study the cyclic performance of flexural controlled SRC columns and establish the flexure and deformation capacities and backbone curves for such columns. Two large-scale SRC columns were constructed with the concrete dimensions and steel details depicted in Fig.1. Specimen transverse reinforcement comprised 90 degree hook hoops spaced at 75 mm. The specimen matrix and material properties are shown in Table 1. The specimens were tested in single curvature bending with two axial load ratios (ALR) of 15% and 80%. The ALR is the ratio between axial load and the gross concrete section capacity based on cylinder compressive strength.

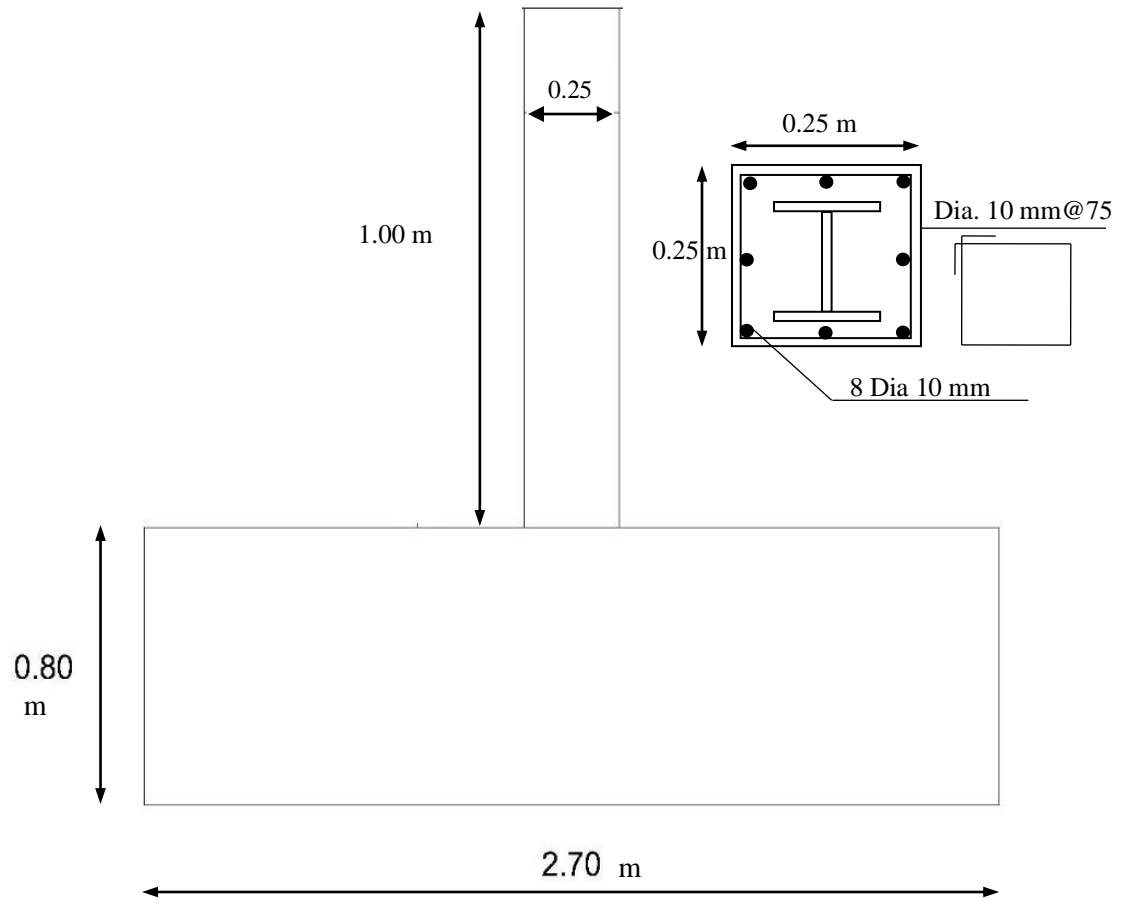


Figure 1: Test specimen details

Table 1: Specimens test matrix

Specimen ID	f_c' MPa	Target Failure Mode	ALR	Hoop Spacing	Steel Section Ratio	Reinforcement Steel Ratio
F15	27.9	Flexural tension	0.15	S=75 mm	5.44% (H120)	1% (8 Φ 10)
F80	27.6	Flexural compression	0.80	S=75 mm	5.44% (H120)	1% (8 Φ 10)

3. Test Setup and Loading Protocol

The test setup comprises a horizontal 220 kN dynamic actuator with a 120 mm tension and compression stroke capacities supported to a strong wall and applying lateral load at the top of the specimen as shown in Fig. 2. The lateral loading rate was 0.5 mm per second. A 2000 kN vertical load cell connected to a vertical jack that is attached to a loading frame and braced laterally to the reaction wall was used to apply the axial load. A rolling mechanism was introduced to allow for sliding of the column top under the vertical load. The test setup is shown in Fig. 3. The test was performed under quasi-static displacement controlled protocol until lateral failure followed by axial failure are reached. The displacement protocol was derived based on multiples of the theoretical yield displacement and is shown in Fig. 4. Two displacement cycles were used prior to reaching theoretical yield displacement followed by three cycles per each displacement amplitude after reaching the theoretical yield displacement. The yield displacement for flexural controlled specimens is calculated by summation of slip, plastic and elastic displacements at section yield predicted via moment-curvature analysis using XTRACT section analysis software. Seven strain gages and seven LVDTs were used to instrument each test specimen at critical strain and displacement locations. A data controller and acquisition systems were used to apply and monitor loading conditions and collect the test data results.

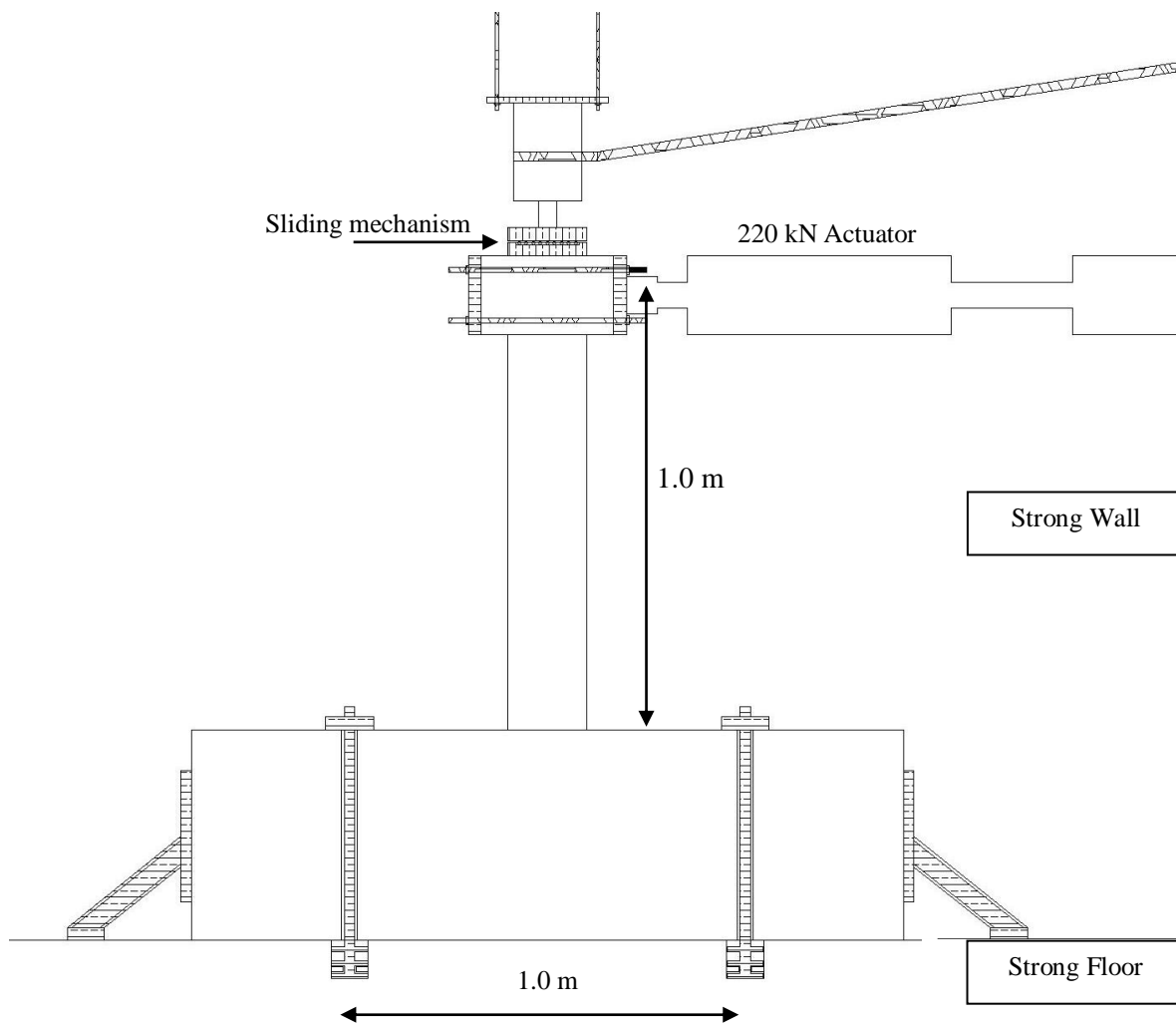


Figure 2: Test setup



Figure 3: Test specimen and setup

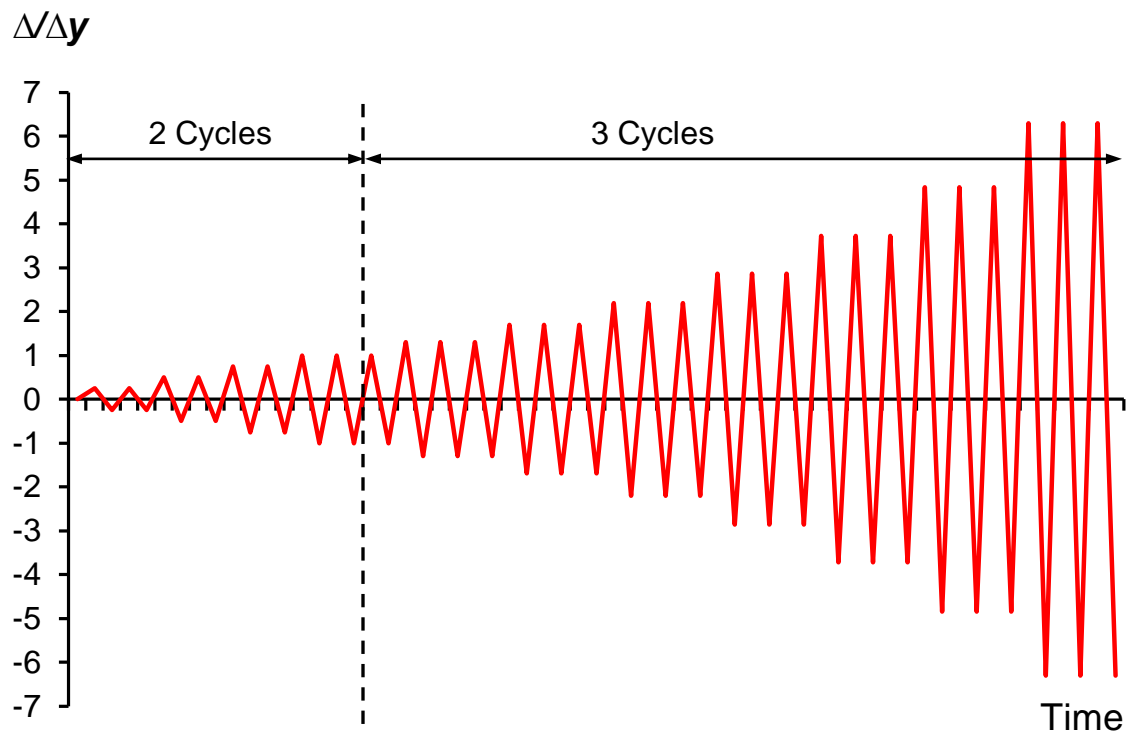


Figure 4: Displacement protocol

4. Experimental Results

Figure 5 shows the failure mode of specimen F15 under the effect of the applied displacement protocol and a constant axial load ratio of 15%. Flexure cracks appeared as early as 0.7% drift ratio. Flexure cracks then progressed on two opposite sides of the specimens especially cracks located in the area of $d/2$ from base of column. The major cracks width kept increasing as the specimen strain-hardened then the specimen started having compression zone spalling and lost its lateral load capacity. One longitudinal bar in each direction of loading ruptured. The test was continued until axial failure was reached, which was identified by severe concrete spalling, buckling of longitudinal bars (with or without buckling of steel section flanges), out-of-plane lateral torsional buckling, opening of hoops and significant sudden loss of vertical axial load (more than 30% loss) .



Figure 5: Failure mode of specimen F15

Figure 6 shows the shear force-drift ratio hysteresis response of specimen F15. The peak shear capacity of the specimen was 161 kN. This exceeded the theoretically predicted flexural capacity of 111 kN. The peak shear capacity was reached at 4.6% drift ratio. The test was continued until 6.1% drift ratio, at which axial failure was identified. This drift ratio is considered relatively high for the typical reinforced concrete existing buildings (with conventional concrete columns) which generally can tolerate less than 2% drift before collapse. The 4.6% peak lateral load drift capacity is considered satisfactory if judged by TBI 2011 acceptance criteria for modern columns under Maximum Considered Earthquake (MCE) single record which is 4.5% and significantly acceptable if compared to the mean MCE acceptance criteria for several records which is 3%. This indicates there is no need to retrofit such columns to meet modern code acceptance criteria. The unsymmetrical post-peak degradation in the positive and negative loading directions is resulted from the fact the initial loading in the positive direction compromise the stiffness of the specimen in negative loading direction as well.

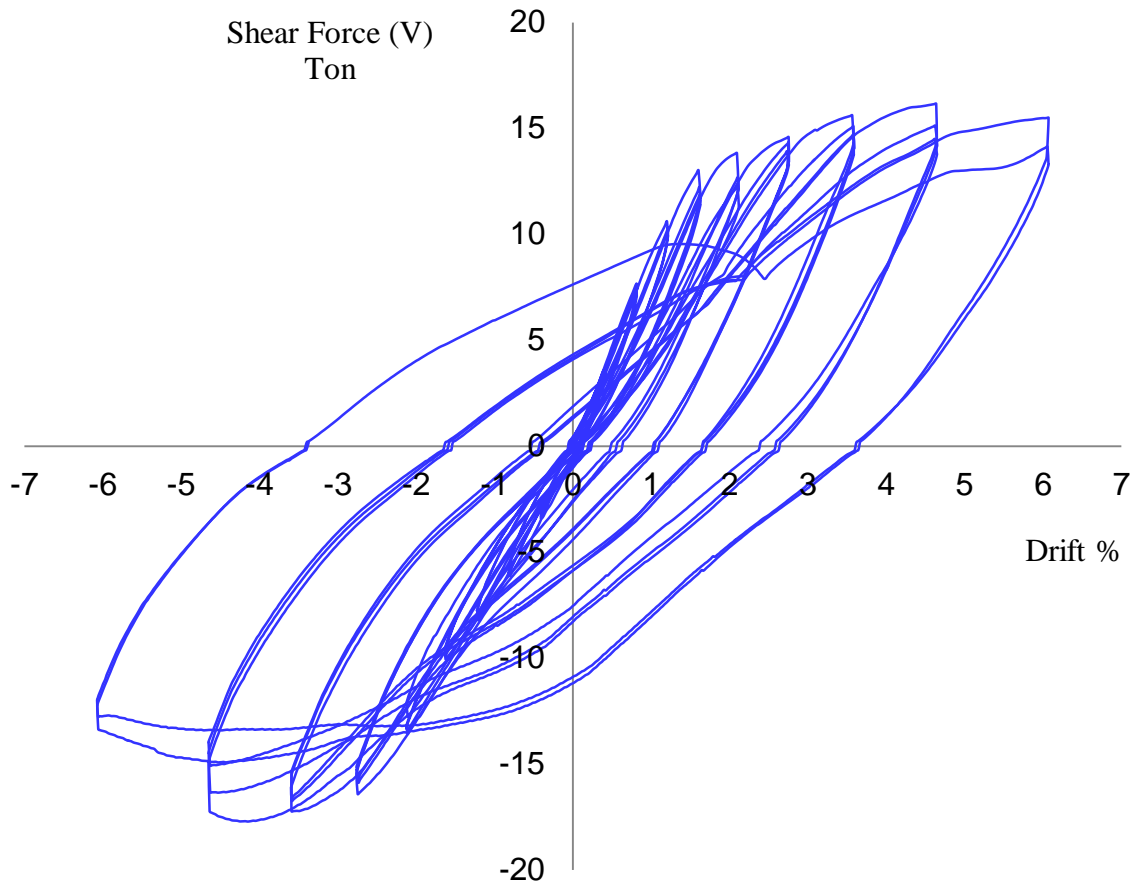


Figure 6: Shear force-drift hysteresis response of specimen F15

The axial failure was reached at 6.1% drift ratio when the axial stability was lost due to rupture of two longitudinal steel bars and buckling of the remaining longitudinal bars. Thus, drift capacity corresponding to axial load ratio of 15% was 6.1%.

Figure 7 shows the failure mode of specimen F80 under the effect of the applied displacement protocol associated with constant axial load ratio of 80%. The failure mode of specimen was a confirmed flexural compression failure characterized by minor flexural cracking on tension sides of the specimen with sudden concrete spalling in the compression zone followed by longitudinal bar buckling and steel section flange buckling in a mode that is similar to that of longitudinal bars. The opening of the 90 degree transverse hoops was very evident which led to crushing in the core concrete. The axial failure was identified at 3.5% drift ratio, when lateral torsional buckling of steel section causing out of plane deformations along with severe concrete crushing and buckling of steel longitudinal bars were reached.



Figure 7: Failure mode of specimen F80

Figure 8 shows the shear force-drift ratio hysteresis response of specimen F80. The peak strength reached was 178 kN which is higher than the 128 kN theoretically predicted strength using XTRACT. The loading stiffness of specimen F80 is obviously higher than that of specimen F15 as can be clearly observed from Fig. 9, which shows the backbone curves of the two specimens in the positive (initial) loading direction. This is attributed to the higher axial load ratio effect in increasing axial stiffness. The peak strength was reached at 2% drift ratio, which is about 57% less than that of specimen F15, emphasizing the effect of higher axial load in limiting the deformability and energy dissipation of the test specimen. This can be also observed by comparing the characteristic fatness of the pre-peak hysteresis loops in specimen F15 indicating flexural tension yielding compared to the narrow ones in specimen F80 suggested more axially driven behavior. Moreover, the axial failure drift capacity of specimen F80 was 3.5% which is about 43% less than the 6.1% axial failure drift capacity of specimen F15. This further indicates the limited seismic deformation capacity imposed by the higher axial load in F80 specimen. The post-peak strength degradation in specimen F80 is much more pronounced than that of specimen F15 confirming the same observation. The highly flattened hysteretic loops in specimen F80 following the axial failure characterize that the specimen response is driven by the steel section residual capacity following out-of-plane deformations. Comparing the drift ratio at the onset of lateral strength loss (2%) to the MCE acceptance criteria of TBI 2011 (3% for the mean of a ground motion suite) indicates the limited deformability and the proneness to collapse of SRC columns in existing buildings with a strong seismic event. This suggests the need to retrofit existing SRC columns with high axial ratios. The unsymmetrical hysteresis loops following loss of lateral strength is resulted from the unsymmetrical loss of concrete compression zone and the out-of-plane buckling deformation of the steel section which is inherently unsymmetrical.

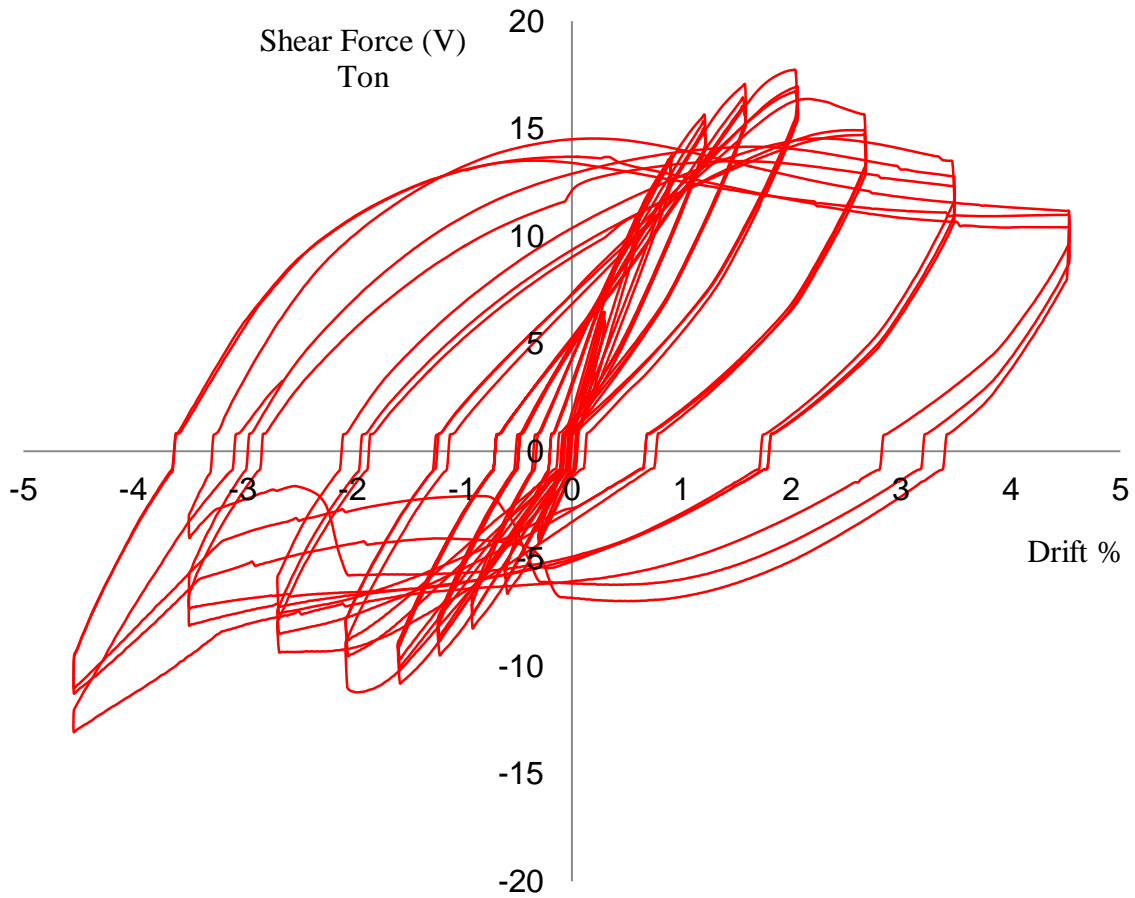


Figure 8: Shear force-drift ratio hysteresis response of specimen F80

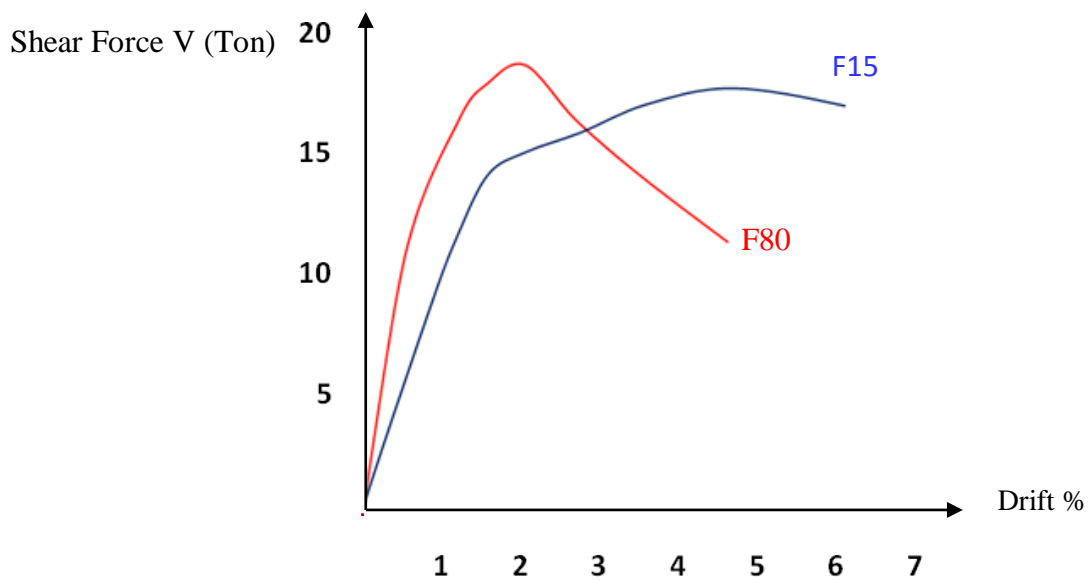


Figure 9: Backbone curves of test specimens



5. Conclusions

Based on the observation of failure modes and test results, the following conclusions can be drawn:

1. The deformation capacity of flexural tension controlled existing SRC columns lacking seismic details with low axial load ratios (15%) is satisfactory even compared to modern building acceptance criteria and may survive strong seismic event since the onset of losing lateral strength was 4.6% drift ratio and the axial failure was reached at 6.1% drift ratio.
2. The flexural compression controlled existing SRC columns with high axial load ratios (80%) are drift-critical since they can lose their lateral strength dramatically as early as 2% drift ratio and can reach axial failure at 3.5% drift ratio. Accordingly, these columns are considered seismically deficient if compared to the modern buildings deformation acceptance criteria.
3. Increasing the axial load ratio from 15% to 80% shows a significantly different failure mode as the high axial load ratio led to the compression zone spalling, buckling of longitudinal bars and steel section flanges and opening the transverse hoops.
4. Increasing the axial load ratio from 15% to 80% was detrimental to deformation capacity of test specimens. It reduced peak shear drift by 57%, axial failure drift by 43% and resulted in faster post peak strength degradation.

6. References

1. ACI 318-63. Building Code Requirements for Structural Concrete, American Concrete Institute, MI, USA.
2. ACI 318-14. Building Code Requirements for Structural Concrete, American Concrete Institute, MI, USA.
3. AISC 341-08. Specification for Seismic Design of Structural Steel, American Institute for Steel Construction, USA.
4. Chen, C., Wang, C., Sun, H., 2014. Experimental Study on Seismic Behavior of Full Encased Steel-Concrete Composite Columns, ASCE Journal of Structural Engineering, Vol. 140, No. 6,
5. Farag, M., and Hassan, W. 2015. Seismic Performance of Steel Reinforced Concrete Composite Columns, 10th Pacific Conference on Earthquake Engineering, Nov. 6-8, Sydney, Australia.
6. Hassan W., and Farag, M., 2017. Seismic Performance of Shear Controlled Steel Reinforced Concrete Composite Columns in Existing Buildings, 16th World Conference on Earthquake Engineering, Jan 9-13, Santiago, Chile.
7. Hassan W., and Farag, M., 2016. Cyclic Performance Assessment of Seismically Deficient SRC Composite Columns, 16th International Conference on Structural Faults and Repair, May 17-19, Edinburgh, Scotland, UK.
8. Hassan, W. M., 2011. Analytical and Experimental Assessment of Seismic Vulnerability of Beam-Column Joints without Transverse Reinforcement in Concrete Buildings. PhD Dissertation, University of California, Berkeley.
9. Ricle, J., and Paboojian, S. 1992. Experimental Study of Composite Columns Subjected to Seismic Loading Conditions. 10th World Conference on Earthquake Engineering, Balkema, Rotterdam.
10. Sezen, H. 2000, Seismic Behavior and Modeling of Reinforced Concrete Building Columns, PEER Report 2000/09, Pacific Earthquake Engineering Research Center, Berkeley, CA, USA.
11. Sarkisian, M., Long, E. D. and Hassan, W. M., 2013. Performance-Based Engineering of Core Wall Tall Buildings, Proceedings, ASCE Structures Congress, Pittsburg, PA, USA.
12. Tall Building Initiative, 2011, Pacific Earthquake Engineering Research Center, University of California, Berkeley, CA, USA.